Int. J. Adv. Eng. Pure Sci. 2020, 32(2): 118-127
DOI: 10.7240/jeps.526906

RESEARCH ARTICLE / ARAŞTIRMA MAKALESİ

A Quantitative Study on the Earthquake Forecast Verification for the Northwestern Turkey

Kuzeybatı Türkiye için Deprem Tahminleri Doğrulama Çalışması

Hakan KARACA[1]

[1]*Nigde Ömer Halisdemir Universitesi, Mimarlık Bölümü 51100, Niğde, Türkiye*

Abstract
Seismic events have a pattern of recurrence in magnitude, time and space. Considerable effort is being spent to identify seismic patterns and successfully predict future earthquakes by using the recognized patterns. As a result of these intensive efforts, a variety of methods has been proposed. As the knowledge and experience in the field accumulated in parallel to the variety of the methods proposed, it was deemed necessary to test the performance of some of the highlighted methods, especially considering the wide reception of methods utilizing SSS, PI and RI. The performance of these methods in forecasting the earthquakes has been selected for investigation.

The investigated area is the region bounded by 27^0-32^0E in longitudes and 39.8^0-42^0N in latitudes, well known for the North Anatolian Fault. The period of coverage has been selected such as to maximize the length with the minimum magnitude of completeness. As a result of such optimization, the period from 1973 to 2019 has been selected with minimum magnitude of completeness being determined as 3.8. In order to measure the relative performance of the methods, ROC analysis has been utilized. The method based on SSS has been adapted to the related ROC procedures, while the results of PI and RI methods are already suitable for the evaluation by ROC procedures.

After the analysis was completed, according to the ROC procedures, none of the methods were singled out in forecast performance. However, when the ratio of hits versus total alarms and the area covered by the alarms, PI method outperforms two other methods by its efficiency.
Keywords: Pattern informatics, relative intensity, earthquake forecast, Northern Anatolian Fault Zone

Öz
Sismik hareketler büyüklük, zaman ve oluşum yerleri bağlamında bir düzende oluşurlar. Bu hareketliliğin hangi düzende ve sırada oluştuğu belirlenerek geleceğe yönelik tahminlerin başarılı biçimde yapılabilmesi için önemli ölçüde çaba harcanmaktadır. Bu çabaların sonucu olarak, şu ana kadar birçok yöntem geliştirilmiştir. Geliştirilen yöntemlerin çeşitliliği bağlamında bilgi ve deneyim artışı süregelmiş ve özellikle çoğunlukla kabul gören yöntemlerden, düzleştirmeye dayalı yöntemler (spatially-smoothed seismicity), örüntü bilişim (pattern informatics) ve göreli yoğunluk (relative intensity) yöntemlerinin yeni verilerle denenmesi gerekli olmuştur. Bahsi geçen yöntemler bu çalışma kapsamında, , deprem tahmin performansları açısından incelenmek üzere seçilmiştir.

27^0-33^0 boylam ve 39.8^0-41^0 enlemleri arasında kalan, Kuzey Anadolu Fay Hattı ile ünlenen bölgemiz, çalışma alanı olarak belirlenmiştir. Çalışma döneminin belirlenmesi için minimum deprem büyüklüğü ile tamlık ölçütlerini sağlayan en uzun dönem araştırılmıştır. Bu kapsamda yapılan analiz sonucuna göre, tamlık ölçütünü sağlayan en küçük deprem büyüklüğü 3.8 olarak bulunmuş, tamlık ölçütlerine uyan dönem ise 1973 ile 2019 yılları arasında kalan dönem olarak belirlenmiştir. Tahmin yöntemlerinin başarısı ise göreli işletim ölçütü (ROC) analizi kullanılarak değerlendirilmiştir. Düzleştirme yöntemi uygulamaları ROC veri girdisi formatına göre uyarlanmış olup, PI ev RI yöntemleri is halihazırda ROC girdilerine uygun olarak veri üretmekte olduğundan herhangi bir uyarlamaya gerek kalmamıştır. Çözümlemeler ve ROC değerlendirmeleri sonucunda yöntemlerden hiçbirisi öne çıkmamış ancak, başarılı tahminlerin toplam tahminlere ve tahminlerin kapladıkları alanlara göre değerlendirmesi sonucunda PI yönteminin diğer iki yönteme göre daha verimli bir yöntem olduğu belirlenmiştir.
Anahtar Kelimeler: Örüntü bilişim, göreli yoğunluk, deprem tahminleri, Kuzey Anadolu fay hattı

Corresponding Author: Hakan KARACA, Tel: (506) 235 1837, e-posta: hakan.karaca@ohu.edu.tr
Submitted: 14.02.2019, **Revised**: 26.12.2019, **Accepted**: 19.02.2020

I. INTRODUCTION

Recently, earthquake forecasting has become a subject with wide reception in the academic community. As the input in the development of forecasting algorithms, generally the spatio-temporal patterns of the past seismic activity are investigated for a wide region or within identified clusters. Among the renowned forecast studies, the ones within the scope of Regional Earthquake Likelihood Models (RELM) (Werner et al., 2011; Schorlemmer et al., 2010,; Zechar et al., 2013; Helmstetter et al., 2006, 2007, 2014) and the studies using the Pattern Informatics (PI) (Tiampo et al. 2002; Rundle et al. 2002, 2003) and Relative Intensity (RI) methods (Holliday et al. 2005, 2006) are receiving high attention as highlights of the field of earthquake forecasting. RELM techniques are based on spatial smoothing algorithms which is based on the optimization of the smoothing algortihm to forecast future pattern of seismicity. PI quantifies change in seismicity rate whereas RI measures the long-term seismicity forecasting in the considered region. PI method is generally accompanied by also included RI forecast models as the reference model.

Among the three mentioned models, the SSS model is mostly derived from the RELM techniques which repeatedly were employed by the listed researchers above. For the purpose of the study, the mentioned techniques are modified so that the associated spatial smoothing algorithm could be transformed into an alarm based forecast. Similar to the RELM techniques, the determination of the smoothing parameters, the log-likelihood method of Kagan and Jackson (1994), is adapted which was later clearly laid out in Helmstetter et al. (2006, 2007). The modified PI method which was laid out by Nanjo (2006) is implemented, as the modified PI proved to be more robust in forecasting. The RI method in its original form is used as a reference model.

Indeed, mainstream ideas lie beneath the forecasting algorithms as being either precursory seismic activation, quiescence or both. All these forecasting algorithms have their roots in the basic idea that large earthquakes tend to occur close to the locations of smaller earthquake clusters (Werner et al., 2011). Hence, by using this assumption, earthquake catalogs, which are generally thought to be missing the large magnitude events due to time gaps between long return periods of large magnitude events and coverage period of the existing catalogs, can be exploited to predict the large magnitude events.

The main issue in comparison of the relative performances of the binary forecasts of PI and RI, and continuum forecast of SSS methods is that a binary forecast specifies whether an event is to occur or not to occur in the interested region, whereas, a continuum forecast offers the likelihood of the event to occur in the interested region (Holliday et al., 2007). In order to compare the performance of the PI, RI and SSS methods, a common measure has to be introduced or adapted. Knowing that SSS methods also rely on the grid system and that the variation of the relative likelihood of event occurrences can be modeled within the grid based system, the likelihood values can be treated as binary forecasts. Only then it is convenient to adapt the Relative Operating Characteristics (ROC) diagram, which indeed is developed to test the binary forecasts. Indeed, it is one of the contributions of this study to evaluate the performance of SSS method in earthquake forecasting. Among the three forecast methods, only the performance of the PI and RI methods are generally tested by using ROC whereas testing of SSS method by ROC is not attempted though it is a quite simple procedure.

In fact, this study is built on the idea that the performance of the various seismic pattern modeling algorithms should be put to the test to identify the outstanding methods. Indeed, depending on the performance of the forecasts, not only it is possible to determine which algorithm performs better but also whether the smoothing algorithm performs better for the interested region. Indeed, the advantage of PI method which considers the past fluctuations of seismicity, over both RI and smoothing methods, is also put to the test by this study as well. The crucial attempt is also made to investigate whether the forecasting methods would had forecasted the devastating earthquakes of Izmit and Duzce that occurred on 17 August 1999 and 12 November 1999. According to the analyses, only Izmit earthquake had precursors that could give hints for a possible future event, whereas since there aren't any precursor events prior to the Duzce earthquake, all the forecasting methods missed the earthquake completely.

II. SEISMIC DATABASE

The area of interest is identified as one of the most tectonically active regions, including the North Anatolian Fault Zone (NAFZ) (Figure 1) which recently has generated Izmit (M_w=7.4) and Duzce earthquakes (M_w=7.2) that caused significant damage. As displayed in Figure 1, the activity is concentrated along northern branch of the NAFZ between the latitudes of 40.5^0N and 41.0^0N. There is also a substantial activity spread over the various locations, as seismic clusters and as sparsely distributed earthquakes at various locations which are not associated with any of the clusters.

.

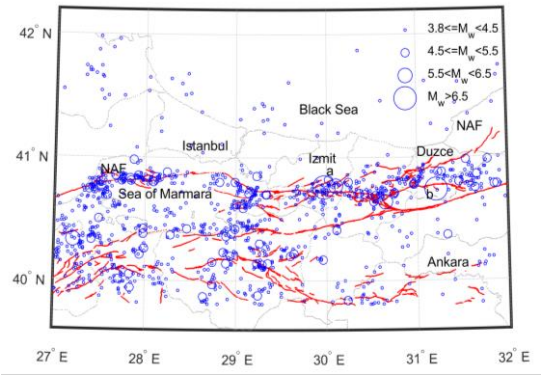


Figure 1. Seismicity around Sea of Marmara (Mw≥3.8, 1973-2019, Declustered, Depth<20 km; a: Izmit Earthquake, b: Duzce Earthquake)

A catalog was created which is composed of KOERI[a] data for the period between 1965 and 2019. The compiled catalog was subjected to homogenization for the purpose of unification of the magnitudes by using local magnitude conversion equations by Akkar et al., 2010, and it was de-clustered by using the time and space windows that were proposed in Gardner and Knopoff (1974). The proposed windows by the mentioned authors developed through a comparative study, which included the comparison of performances of commonly use de-clustering procedures with the Turkish data. Here, it should be mentioned that the de-clustering procedures are used to sort out the main earthquakes which are assumed to follow Poisson distribution. The de-clustering procedure removes the large fluctuations in temporal domain and enable us to identify the long term seismic activity rate. Before de-clustering, 2325 earthquake events were identified within the considered area, whereas, the number of events decreased to 1125 after de-clustering, which indicates the existence of a large number of foreshock and aftershock events in the catalogs.

The determination of the temporal variation of minimum magnitude of completeness (M_c) and the consequent evaluation of the catalog is a must for a reliable analysis. In this study, the method presented in Cao and Gao, 2002 is utilized to identify the values of M_c. As the product of the utilized method, the temporal variation of the Mc is displayed in Figure 2. Accordingly, the longest coverage period is selected as the period between the years of 1973 and 2019 as the M_c is identified as 3.8.

The temporal variation of the M_c is largely caused by the developments in the recording technology as well as the density and distribution of the instrumentation. Hence it is almost unavoidable to have a catalog with the different M_c values for any considered time interval. This variation, which should be a subject of another study, could be attributed to many reasons including the nature of the data itself, the magnitude conversion equations and the data collection procedures with different magnitude scales at different periods (Öztürk (2011, 2017).

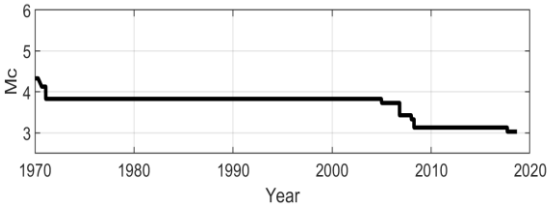


Figure 2. Temporal Variation of Magnitude of Completeness

III. METHOD

The PI method, which is based on monitoring the spatial and temporal variation of seismicity, doesn't provide the precise timing and location of a future seismic event, but provide a relative degree of possible future event locations for a predetermined time frame. Since the method is based on the idea to extrapolate the spatio-temporal pattern into a predetermined future time frame, it is a pre-requisite to identify the fluctuations of past seismic activity. The RI method, on the other hand is based on an approach based on the idea that large earthquakes tend to occur close to the locations of smaller earthquake clusters. Smoothing methods also is based on the same idea as in RI method with the only difference being the smoothing scheme. The detailed formulations are provided in the Appendix of this study.

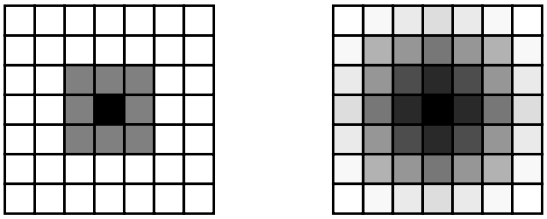


Figure 3. Moore Neighborhood (left) and Simple Smoothing Scheme for SSS Methods (right)

The PI and RI methods generally use a Moore neighborhood technique (Moore, 1962) (Figure 3) which is based on assignment of alarms only to the neighboring cells of the seismically active cell. The SSS method, the smoothing scheme is relatively complicated (Figure 3) to utilize especially for the grid system. As a matter of fact, the SSS methods is expected to enhance the forecast capability as the basic idea of the smoothing methodology is that future earthquakes are expected to occur within a close vicinity of past earthquakes. Moreover, smoothing helps compensate for limitation in the data, and it accounts for uncertainty in the location of the

epicenter. The formulations of PI, RI and smoothing method is provided in detail in the appendix.

Determination of the seismic activity patterns with respect to the space, magnitude, time and depth requires splitting the catalog into different bins. If there is sufficient number of events to detect a recognizable pattern, and an even distribution of events is provided which allow binning of the catalog into different magnitude bins, it is probable that the binning of the catalog with respect to time and magnitude might yield a meaningful pattern.

Table 1. Schemes for the Verification of the PI, RI and SSS methods

Scheme	Training Period	Learning Period	Forecast Period
	Coverage	Coverage	Coverage
1	1973-1999	1999-2009	2009-2019
2	1973-2004	2004-2014	2014-2019
3	1973-2009	2009-2014	2014-2019
4	1973-1989	1989-1999	1999-2000
5	1973-1990	1990-1995	1995-2000
6	1973-1985	1985-1995	1995-2000

In order to model the spatial distribution patterns in a manner best serving to the purpose of this study, the trade off between the loss of meaning by larger binning sizes and pointless division of the area into more grids than just sufficient should be handled delicately (Mohanty et al., 2016). For that reason, the size of the grids is subjectively selected in order to reflect the spatial density of the studied area. Accordingly, for the spatial binning, for all the forecast models, the area of interest is divided into spatial boxes sized 5 km x 5 km, which corresponds to 0.0625^0x0.050^0 grids in longitudes and latitudes. For computational purposes the study area is extended by a single line of grid in both directions.

The temporal variation is measured through splitting the catalog into training and learning periods. In the selection of the periods, it is not forgotten that the time span for the training catalog should be long enough for the detection of the temporal seismic pattern, and the learning part should be sufficiently wide enough to verify the identified pattern.

For the verification of the forecast algorithms and testing the relative performances of each algorithm, six different schemes were developed as seen in Table 1. The first three schemes were planned in order to verify 5 and 10 year forecasts by using varying training and learning periods. The second group of schemes, scheme 4, 5 and 6 were developed to test the capabilities of the methods to forecast the earthquakes of Izmit (M_w=7.6, Aug,17) and Duzce (M_w=7.2, Nov,12) in 1999. For these schemes, 1-year, 5-year and 10-year forecasts were employed and the performances of the PI, RI and SSS methods in forecasting the mentioned earthquakes were monitored. Indeed, the sole purpose of developing these schemes was to observe whether the forecasting algorithms would give an alarm before the devastating earthquake occurred.

In addition to the periods of coverage for each scheme, Table 1 also clarifies the distribution scheme of the events into the different periods also. Among all three schemes, scheme 1 has a more even distribution of events for the training, learning and forecast periods, whereas scheme 3, having the longest training period among the three, has more events lumped into the training period and a lesser number of events for both learning and forecast periods. It should also be mentioned that, the schemes are designed in such a way that, from scheme 1 to 3, the training periods becomes longer while the learning and forecast periods varies in terms of the length.
While the first three schemes are developed to test the forecast performance of the PI, RI and SSS methods, the sole purpose of developing schemes 4, 5 and 6 was to be able to observe whether these methods would have provided clues to the devastating earthquakes of Izmit,1999 and Duzce,1999. Hence the periods of training, learning and forecasting was determined accordingly. In scheme 4, a long term forecast was performed at the start of year 1999 whereas in schemes 5 and 6, a 5-year forecast was specifically planned to test the predictability of the devastating earthquakes of 1999.

After setting up the forecast schemes, the performance of the methods in forecasting is tested by ROC, selected from amongst the several techniques available for the evaluation of forecast (Kagan and Jackson, 1994, Molchan, 1997, Mason, 2003). ROC curves are extensively used in many fields that employ forecast systems and require assessment of the quality of the forecasts. The curve is constructed through the assessment of the quality of the forecast at predefined threshold levels.

In order to generate these curves, the hit rate, in other words, the ratio of the number of successfully forecasted events to the total observed events at the predefined threshold, is plotted against the false alarm rate - the rate of the number of events incorrectly forecasted to the total number spots where no earthquake is observed. The performance of each method for each forecast scheme is comparatively evaluated with respect to the slope of the hit rates and false alarm rates. The slopes at the initial threshold level (Θ_i) and the average slope (Θ_f) of the ROC curves are compared. The average slope is assumed to be the final values of hit rates divided by the final false alarm rates. Another tool used to evaluate the performance of the forecasts, is the contingency table. The table is generated to display the number of

successful forecasts or hits and failed forecasts or false alarms with respect to the observations. Misses, or number of occurred earthquakes that weren't forecasted and correct negatives or successfully forecasted silent spots where no earthquakes occurred are also listed in the table.

IV. RESULTS

As the fist step towards the analysis, forecast maps for all the schemes were generated to locate the hotspots where the earthquakes are likely to occur within the forecast period. In order to give an example, for scheme 1, the hotspots can be seen in Figure 4, where earthquakes are likely to occur within the period covering 2009-2019. According to the figure, the number of hotspots or alarms where the probable location of future earthquakes are significantly fewer with the PI method whereas RI and SSS methods forecast a considerably higher number of events. Secondly, the PI and RI values display a scattered pattern across the areas of interest, whereas the SSS method lumps the hotspots into more compact areas. Indeed, the lumping characteristic of the SSS method might be a limiting factor in the capacity to forecast future events. For example, in the areas north of Ankara, these methods do not foresee any future event, which PI and RI methods did successfully forecast.

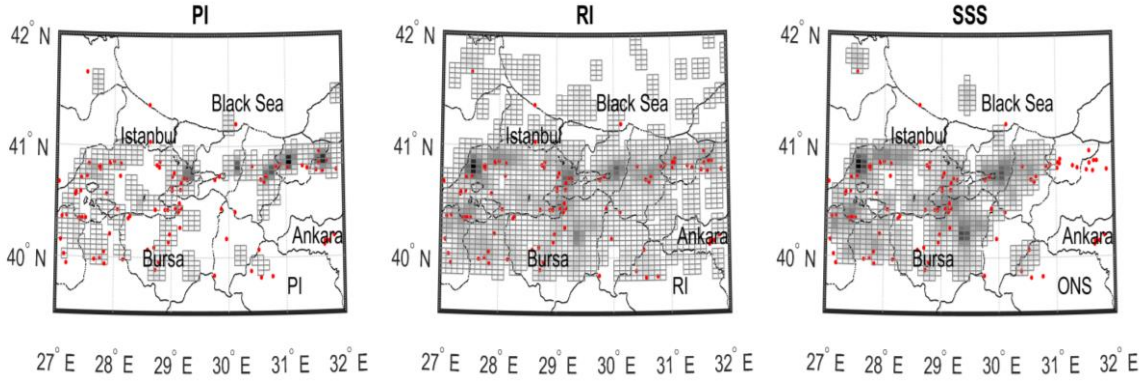


Figure 4. The Forecast Map for the Scheme 1 (The Probability of Earthquake Occurrence Increases with Color, Dots are Observed Earthquakes for 2009-2019 with $M_w \geq 3.8$)

Due to space requirements, other forecast maps couldn't be provided; however, the ROC curves are created as a measure of performance for each scheme. Figure 5 presents the curves, for the visual examination of the relative performances of each algorithm. In the figure the green line represents random guess which can be used as reference to measure the relative success of the schemes. Interestingly, while all the curves are well above green line, none of the method can be singled out for outstanding performance except for the slightly better performance of PI method for schemes 1 to 3.

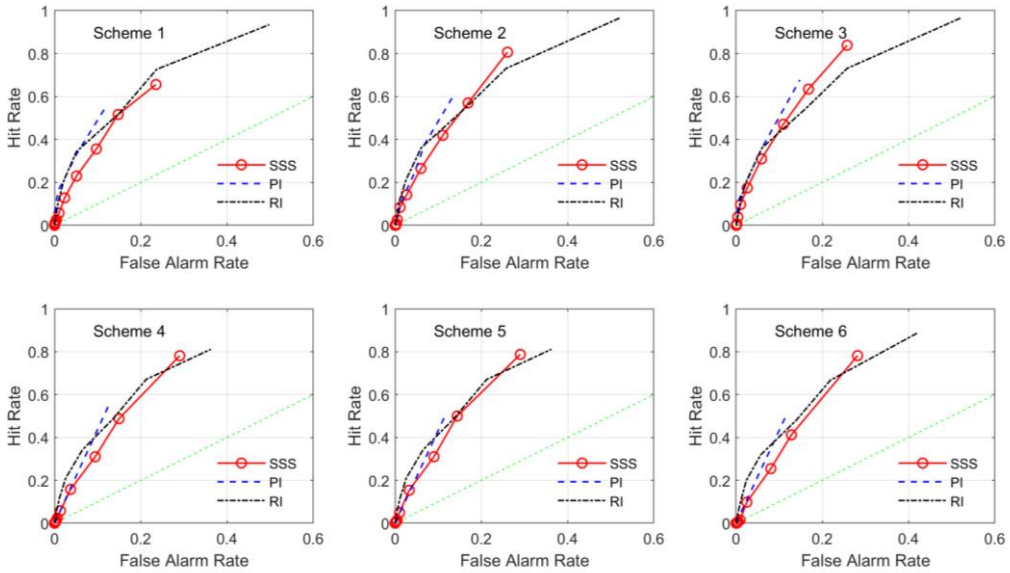


Figure 5. The Hit Rate versus False Alarm Rate for all the Schemes

After visual examination, it is easily concluded that the qualitative approach doesn't yield any reliable results, due to the absence of relatively outstanding performance. For quantitative analysis, only the initial and average slopes of these ROC curves in Table 2, offer information about the varying performances of the utilized methods. Especially higher initial and average slopes of PI curves deserve to be mentioned for schemes 1 to 3, indicating better performance of this method in forecasting. For schemes 4 to 6, initially RI display superior performance then the rest whereas overall performance of PI exceeds the other two methods as well. The performance of SSS method generally lag behind both the PI and RI, except for the overall performance of RI method.

Table 2. Initial and Overall Slopes of ROC Curves of Schemes

	PI		RI		SSS		Length of Periods		
Schemes	Θ_i	Θ_f	Θ_i	Θ_f	Θ_i	Θ_f	Train	Learn	Test
1	46.46	4.68	30.98	1.88	30.98	2.79	26	10	10
2	24.97	4.44	15.61	1.85	5.00	3.09	31	10	5
3	24.97	4.57	15.61	1.85	7.34	3.26	36	5	5
4	4.38	4.37	11.77	2.24	3.90	2.69	16	10	1
5	4.32	4.31	11.77	2.24	7.79	2.71	17	5	5
6	11.87	4.70	16.44	2.11	3.18	2.77	12	10	5

Θ_i: Initial slope, Θ_f: Average slope

The contingency table is referred for better assessment of the results, as the table is populated with the analyses results for each method and scheme in a compact manner in Table 3. Before a detailed examination, it should be mentioned that, in order to compute the number of hits, false alarms, misses and correct negatives of the table, for PI and RI methods, positive values are accepted as hot spots where the earthquakes are forecasted to occur while the values above the average is accepted as hot spots for SSS method. At first the higher number of false alarms of PI gets the attention as both RI and SSS methods seems higher rate of hits and lesser false alarms, whereas if the number of hot spots are considered, RI method significantly outperform the others distantly followed by the SSS method. The correct negatives are the highest in all the schemes for all the methods except for the schemes 1 to 3 for RI method as the number of silent spots are outnumber the seismic events. It should be reminded that, the partitioning of the area into a number of spatial bins is also a determining factor for the number of silent spots. Indeed, if the number of spatial bins is reduced, a higher forecast performance could be expected.

Considering that the training periods of the schemes of 1, 2 and 3 are intentionally increased in order to observe the influence of the length of the training period over the forecast, it is expected to have varying performances with respect to the changing period length. As a matter of fact, there is an emerging pattern from amongst the initial slopes of the curves, which paves the way to associate the relative performances of schemes 1, 2 and 3 with the subjective partitioning of the catalog. The initial slopes of the ROC curves of all the methods are considerably higher for scheme 1, with PI values being significantly higher than those of the others. Combining with the success trend of PI in schemes 2 and 3, the results indicate the clustering of events at different locations in time.

Table 3. Contingency Table for the Forecast Schemes*

Scheme			FORECASTED					
	Hit	Miss	PI		RI		SSS	
	False alarm	Correct Negative	Yes	No	Yes	No	Yes	No
1	OBSERVED	Yes	66	56	115	7	80	42
		No	440	3339	1933	1846	909	2870
2		Yes	19	12	30	1	25	6
		No	545	3325	2069	1801	1026	2844
3		Yes	20	11	30	1	25	6
		No	575	3295	2069	1081	1011	2859
4		Yes	31	26	52	5	43	15
		No	437	3407	1680	2164	1063	2780
5		Yes	80	85	66	99	128	38
		No	437	3299	192	3544	1069	2666
6		Yes	92	73	66	99	127	39
		No	481	3255	192	3544	1045	2960

** The number of boxes is 3901 for all the schemes as the considered area is extended single line of grid in both directions.*

Regarding testing the performance of forecast algorithms on the prediction of the two big earthquakes of Izmit and Duzce in 1999, schemes 4, 5 and 6 were developed. Indeed, the schemes are specifically developed as one of the crucial objectives of the study is to verify the principle which states that large earthquakes tend to occur close to the locations of smaller earthquake clusters. Indeed, according to Figure 6 that is prepared to display the alarm map and forecasted earthquakes of scheme 4, there is a significant seismicity accumulated within the close vicinity of Izmit earthquake, whereas the areas close to the epicenter of Duzce earthquake is relatively silent, a fact that has a direct influence on the outcome of the performance comparison.

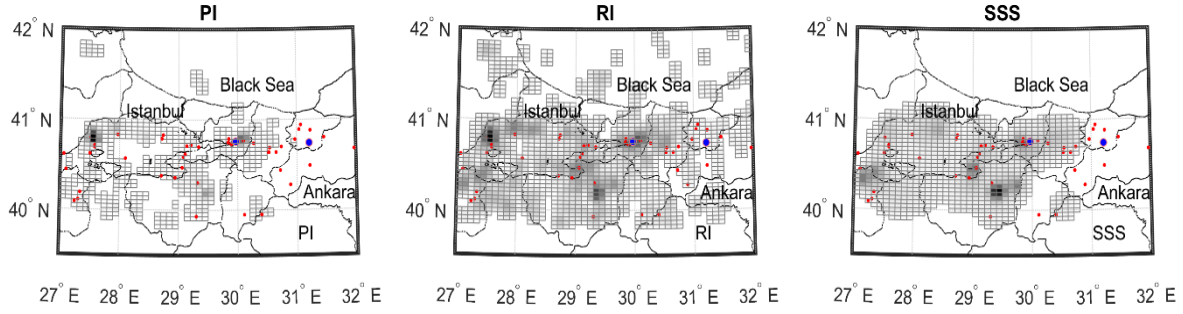


Figure 6. The Forecast Map for the Scheme 6 (The Probability of Earthquake Occurrence Increases with Color, Dots are Observed Earthquakes for 1999-2000 with $M_w \geq 3.8$)

Table 4. Varying Alarm Rates (The Area of Alarm/Total Area) at the Successful Forecast of for Izmit and Duzce Earthquakes

	Izmit			Duzce		
	PI	**RI**	**SSS**	**PI**	**RI**	**SSS**
Scheme 4	0.54	0.62	0.17	0.00		
Scheme 5	0.56	0.45	0.21			
Scheme 6	0.22	0.45	0.10			

As a matter of fact, the evaluation of the performances of each method is conducted as the ratio of the probability of occurrence of an earthquake at the epicenters of the Izmit and Duzce earthquakes, is computed with respect to the highest probability throughout the whole area. The computed ratio between the two probabilities is proportional to the alarm rate as well. In other words, as the ratio becomes higher, the alarm rate or the probability of occurrence is relatively higher as well. In light of above explanations, Table 4 was created for the evaluation of the relative performances of each method and scheme. Clearly, all of the methods and schemes completely miss the Duzce event, which indeed raise questions about the basic principle about the occurrences of large earthquake. For the Izmit earthquake, both PI and RI methods are more successful in scheme 4, whereas SSS method display lower performance in all the schemes.

Another aspect of the forecast performance is also checked to account for the high variability of the number of hot spots or alarms of each method and scheme. So, the forecast success rate, or the ratio of the successful forecasts to the number of hot spots or alarms are plotted against the schemes and the percentage of area of alarms. As can be seen in Figure 7, except for the schemes 5 and 6, there is a wide gap between the performance of each method with respect to the mentioned measures. PI method outperforms the other two by a significant margin by lesser number of alarms and higher number of hits per alarm and per the percentage of area of alarms as well.

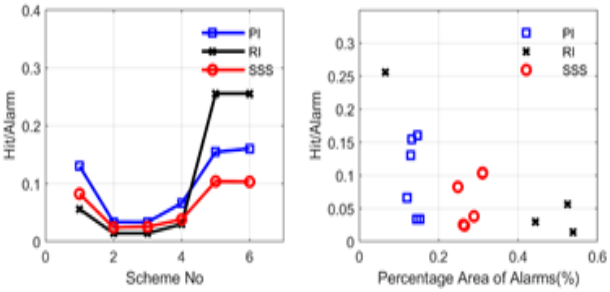


Figure 7. Forecast Success Rates of Each Methods with Respect to each Scheme and Forecast Area Ratio

V. DISCUSSION AND CONCLUSION

Knowing that the mentioned methods are developed based on the variety of seismicity patterns, it is expected that for an area with sufficient seismic information, a well-formulated forecast study would yield satisfactory results. In the case of a failure, either the formulation of the forecast scheme would be questioned or the non-conforming seismic patterns of the area of interest. However, if there are seismic patterns in the area of interest that don't comply with the assumptions of the forecast algorithms, then the approach should be modified. In this study, though

the forecast performance is well above random chance, it should be admitted that it yielded a moderate result.

One of the significant results that could be drawn from this study is that Indeed, as displayed in Figure 7, PI method performed slightly better by the common measures and by wide margin with respect to the measures introduced within this study. Having a pattern of seismicity as in the considered region, it could be projected that at some point in the future, it might be possible to forecast future events with more precision only with the condition that if the past fluctuations of seismicity could be better modeled. RI and SSS methods, having based on the idea that future events are more likely to occur within the close vicinity of the locations of past earthquakes regardless of its temporal distribution, are inherently incompetent. While according to the ROC curves and associated values derived from these curves, the performances of these methods are not very low compared to PI method. However, the number of hotspots or alarms are so high, both methods almost consider the whole interested area as hotspots in some cases, an inefficiency causing these methods to be less attractive.

Last but not least, the reason why SSS method performs better than RI while couldn't match with the performance of PI (Figure 7), lies within the fact that SSS lumps the alarms into more compact form in contrast to RI method which spread out the hotspots to entire area. The lumping of the seismicity assists in forecasting the future events as the identified seismic sources are expected to generate seismic events in the future, which holds true despite the fact that seismic clusters might be formed in different areas at different times as in the case of clustering around Düzce earthquake after 1999.

As a common sense, it is expected that, the capability to foresee future events would more likely to be increased as the accumulation of seismic events would offer more hints about the inherent seismic behavior of the area. Actually, the influence of the length of the catalog and subjective partitioning of the catalog into the periods of training, learning and forecasting is the sole determining factor in forecasting. Which scheme would perform better depends entirely on the seismic pattern of the interested region (Tiampo et al. 2007, Öztürk, 2014, Mohanty et al., 2016). Hence, it is always clever to evaluate the future seismicity of the interested area with several schemes and assess the performance and the forecast capability of the methods with several schemes as well (Tiampo and Shcherbakov, 2011, Zechar, 2010).

In the lights of above discussions, one might reach to the conclusion that the forecast algorithms, being susceptible to the spatio-temporal pattern of seismicity, and binning methodology, might differ in forecast performance. Inherently, in a location with highly clustered seismicity and even temporal distribution, all the methods are expected to perform well, whereas, in a seismically active area with large variation in seismic pattern, PI method is expected to perform better (Holliday et al., 2005, Nanjo et al., 2006, Zechar and Jordan, 2008, Chen, 2011, Mohanty et al., 2016) as is the case with this study. Hence, it could be stated that seismicity has different sensitivities that different methods could identify better than the others. However, it should also be mentioned that accumulation of seismicity through time might eventually allow the determination of the best performing method in modeling the seismicity.

REFERENCES

Kitaplar

[1] Mason, I.B. (2003). Binary events. In Forecast Verification, I. Jolliffe I. and D.B. Stephenson (ed)), Wiley, Chichester, England, s 37–76

Makaleler

[1] Werner, M.J., Helmstetter, A., Jackson, D.D. ve Kagan, Y.Y. (2011). High-Resolution long-term and short-term earthquake forecasts for California, Bull Seism Soc Am., 101(4), 1630–1648

[2] Schorlemmer, D., Zechar, J.D., ve RELM Working Group. (2010) First results of the Regional Earthquake Likelihood Models experiment, Pure Appl Geophys, 167, 859-876

[3] Zechar, J.D., Schorlemmer, D.,Werner, M.J., Gerstenberger, M.C., Rhoades, D.A. ve Jordan, T.H. (2013). Regional Earthquake Likelihood Models I: First order results, Bull Seism Soc Am., 103(2A), 787–798.

[4] Helmstetter, A., Kagan, Y.Y. ve Jackson, D.D. (2006). Comparison of short-term and time-independent earthquake forecast models for Southern California, Bull Seism Soc Am., 96(1), 90-106.

[5] Helmstetter, A., Kagan, Y.Y. ve Jackson, D.D. (2007). High-Resolution time-independent grid-based forecast for M ≥ 5 earthquakes In California, Seismol Res Lett., 78(1),78–86.

[6] Helmstetter, A. ve Werner, J.M. (2014). Adaptive smoothing of seismicity in time, space and magnitude for time-dependent earthquake forecasts for California, Bull Seism Soc Am., 104(2), 809-822.

[7] Tiampo, K.F., Rundle, J.B., McGinnis, S., Gross, S.J. ve Klein, W. (2002). Mean field threshold systems and earthquakes: An application to earthquake fault systems. Europhys. Lett., 60(3):481–487.

[8] Rundle, J. B., Turcotte, D. L., Shcherbakov, R., Klein, W., ve Sammis, C. (2003). Statistical physics approach to understanding the multiscale

dynamics of earthquake fault systems. Rev. Geophys., 41(4),1019.

[9] Holliday, J.R., Nanjo, K.Z., Tiampo, K.F., Rundle, J.B. ve Turcotte, D.L. (2005). Earthquake forecasting and its verification. Nonlinear Processes Geophys., 12, 965–977.

[10] Holliday, J.R., Rundle, J.B., Tiampo, K.F., Klein, W. ve Donnellan, A. (2006). Modification of the Pattern Informatics method for forecasting large earthquake events using complex eigenvectors. Tectonophysics. 413(1–2), 87–91.

[11] Kagan, Y.Y. ve Jackson, D. (1994). Long-term probabilistic forecasting of earthquakes. J Geophys Res. 99(B7), 13685–13700.

[12] Nanjo, K.Z., Holliday, J.R., Chen, C.C., Rundle, J.B. ve Turcotte, D.L. (2006). Application of a modified pattern informatics method to forecasting the locations of future large earthquakes in the central Japan, Tectonophysics, 424, 351-366.

[13] Holliday, J.R., Chen, C.C., Tiempo, K.F., Rundle, J.B., Turcotte, D.L. ve Donnellan, A. (2007). A RELM earthquake forecast based on Pattern Informatics. Seismol Res Lett., 78(1), 87–93.

[14] Akkar, S., Cağnan, Z., Yenier, E., Erdogan, E., Sandıkkaya, M.A. ve Gülkan, P. (2010). The recently compiled Turkish Strong-Motion Database: Preliminary investigation for seismological parameters, J of Seismol., 14, 457-479.

[15] Gardner, J. K., and L. Knopoff (1974), Is the sequence of earthquakes in Southern California, with aftershocks removed, Poissonian?, Bull. Seis. Soc. Am., 64(5), 1363–1367

[16] Cao, A. and Gao, S.S. (2002). Temporal variation of seismic b-values beneath northeastern Japan island arc. Geophys Res Lett 29:

[17] Öztürk, S. (2011). Characteristics of seismic activity in the Western, Central and Eastern Parts of the North Anatolian Fault Zone, Turkey: Temporal and spatial analysis, Acta Geophys., 59 (2), 209-238

[18] Öztürk, S. (2017). Kuzey Anadolu Fay Zonu ve civarındaki güncel deprem aktivitesinin bölgesel ve zamana bağlı analizleri, Yer Bilimleri, 38(2), 193-228

[19] Mohanty, W.K., Mohapatra, A.K., Verma, A.K., Tiampo, K.F. ve Kislay, K. (2016) Earthquake forecasting and its verification in Northeast India, Geomat Nat Haz Risk., 7(1), 194-214

[20] Molchan, G.M. (1997) Earthquake predictions as a decision-making problem, Pure Appl. Geophys., 149, 233–247

[21] Tiampo, K.F., Rundle, J.B., Klein, W., Holliday, J., Martins, J.S. ve Ferguson, C.D. (2007). Ergodicity in natural earthquake fault networks. Phys Rev E., 75,066107

[22] Öztürk, S. (2014). Türkiye'nin Batı Anadolu bölgesi için deprem istatistiği ve olası güçlü depremlerin orta vadede bölgesel olarak tahmini üzerine bir çalışma, Gümüşhane Üniversitesi Fen Bilimleri Enstitüsü Dergisi, 4(1), 75-93

[23] Tiampo, K.F. ve Shcherbakov, R. (2011). Seismicity-based earthquake forecasting techniques: Ten years of progress, Tectonophysics., 522–523, 89–121

[24] Zechar, J.D. (2010) Evaluating earthquake predictions and earthquake forecasts: a guide for students and new researchers, Community Online Resource for Statistical Seismicity Analysis, doi:10.5078/corssa-77337879.

[25] Zechar, J.D. ve Jordan, T.H. (2008) Testing alarm-based earthquake predictions, Geophys. J. Int., 172, 715–724

[26] Chen, C.C. (2011). Characteristics of long-term regional seismicity before the 2008 Wen-Chuan, China, earthquake using pattern informatics and genetic algorithms, Nat Hazards Earth Sys., 11, 1003–1009.

Bildiriler

[1] Moore, E.F.. (1962). Machine models of self reproduction, Proceedings of the Fourteenth symposium on Applied Mathematics; Providence, Richmond, USA, American Mathematical Society.

[2] Rundle, J.B., Tiampo, K.F., Klein, W., Martins, J.S.S. (2002). Self-organization in leaky threshold systems: The influence of nearmean field dynamics and its implications for earthquakes, neurobiology, and forecasting. Proceedings of National Academy of Sciences, U. S. A., 99:2514–2521: Suppl. 1.

Internet

[1] Kandilli Rasathanesi ve Deprem Araştırma Enstitüsü, KOERI (2017) http://www.koeri.boun.edu.tr/sismo/zeqdb/, Last Date of Access: January 2019.

APPENDIX

A.1. PI Method

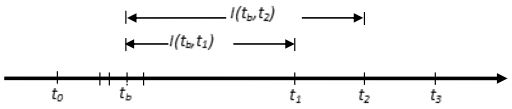


Figure A1 Temporal Range Selection of Earthquake Time Series.

Initially, temporal windows were established to be able to monitor the variation of seismicity. A reference temporal window between t_0 and t_1 and a change temporal window between t_1 and t_2 were established to be able to detect the variation of seismic intensity in time, which led to the necessary information to forecast earthquakes in the forecast window between t_2 and t_3. The introduction of base time, t_b, which moves from t_0 to t_1, is required to

monitor the seismic variation, which indeed is the difference between the normalized seismic density over the time from t_b to t_2, $I(t_b, t_2)$ and from t_b to t_1, $I(t_b,t_1)$.

$$\hat{I}_i(t_b,t) = \frac{I_i(t_b,t) - \langle I_i(t_b,t)\rangle}{\sigma(t_b,t)} \quad \text{(A1)}$$

Here $I_i(t_b,t)$ is the seismic density, $\langle I_i(t_b,t)\rangle$, the mean of the seismic density over all the grids, and the spatial standard deviation, $\sigma(t_b,t)$. The variation of seismicity is computed by subtracting the normalized seismic densities

$$\Delta I_i(t_b,t_1,t_2) = \hat{I}_i(t_b,t_2) - \hat{I}_i(t_b,t_1) \quad \text{(A2)}$$

The seismic variation is averaged over the time, from t_0 to t_1, where the base time varies,

$$\overline{\Delta I_i(t_0,t_1,t_2)} = \frac{1}{t_b - t_1}\sum_{t_b=t_0}^{t_1} \Delta I_i(t_b,t_1,t_2) \quad \text{(A3)}$$

Then the probability of a future earthquake for grid i is computed by

$$P_i(t_0,t_1,t_2) = \overline{\Delta I_i(t_0,t_1,t_2)}^2 \quad \text{(A4)}$$

Finally, the spatial mean of the probability is subtracted from the earthquake occurrence probability, in order to identify the hotspots where future seismic events are forecasted to occur.

$$\Delta P_i(t_0,t_1,t_2) = P_i(t_0,t_1,t_2) - \langle P_i(t_0,t_1,t_2)\rangle \quad \text{(A5)}$$

A.2. RI Method

The number of earthquakes for each grid box is counted and the values are normalized by using the maximum of the values of all the grid boxes.

$$n_i(t_0,t_2) = \sum_{t=t_0}^{t_2} n_i(t) \quad \text{(A6)}$$

Here $n_i(t_0,t_2)$ is the number of earthquakes in each grid box between t_0 and t_2. It is a basic assumption that the probability of future earthquakes in each grid box is proportional to the number of earthquakes in each box. The normalization of these values with a maximum number of earthquake counts in the grid boxes just enhances the computation efforts while not influencing the final outcome.

A.3. Smoothing Method

The widely accepted and utilized smoothing algorithm is the simple Gaussian isotropic kernel:

$$K_d(r) = c(D)\exp\left(-\frac{|r|^2}{2D^2}\right) \quad \text{(A7)}$$

Here D is the smoothing distance and $c(D)$ is the normalizing factor. A reverse bell-like shape centered at the earthquake epicenter smears the seismicity rates to the neighboring grids, where the r value is assigned to be the exact distance of a single grid box.

The optimum values for the smoothing distances were introduced when encountering a loss of meaning, blurring of the seismic activity rates or fragmentation of seismic density due to the large or small kernel bandwidths (Stock and Smith, 2002). The method based on the optimum neighbor number (ONS) in setting the smoothing distance doesn't follow the same suit with PI and RI methods, and for each earthquake the optimum kernel bandwidth varies depending on the varying influences of earthquakes in the determination of the right pattern of occurrences. Here the optimum kernel bandwidth is determined by the method based on Kagan and Knophoff (1977). The information gain per each earthquake for varying distances with respect to the reference model is measured by

$$G = \exp\left(\frac{\log(LL) - \log(LL_r)}{N_t}\right) \quad \text{(A8)}$$

Here LL is the log-likelihood of the tested model, and LL_r is the log-likelihood of the reference model. N_t is the total number of earthquakes in the testing catalog. The log-likelihood of a model is determined by the summation of the terms of the Poisson distribution:

$$\log(LL) = \mu_{\min} + \sum_i \log p(\lambda(i_x,i_y),\omega(i_x,i_y)) = \mu_{\min} + \sum_i \left[-\lambda_i + \omega_i \log(\lambda_i) - \log(\omega_i!)\right] \quad \text{(A9)}$$

Above $\mu_{\min}$ is the positive constant parameter to account for seismic noise, p is the occurrence probability. λ_i is the normalized spatial density, and w_i is the number of observed events in the testing catalog for each cell i.